

Macroscale computer simulations to investigate the chemical vapor deposition of thin metal-oxide films

E. Neyts^{a,*}, A. Bogaerts^a, M. De Meyer^{b,c}, S. Van Gils^{b,c}

^a University of Antwerp, Dept. of Chemistry, Plasmant research group, Universiteitsplein 1, 2610 Antwerp, Belgium

^b OCAS, Arcelor Research Industry Ghent, Surface Functionalisation, John Kennedylaan 3, 9060 Zelzate, Belgium

^c Flamac (Flanders Materials Centre), Technologiepark 903, 9052 Zwijnaarde, Belgium

Available online 1 May 2007

Abstract

The chemical vapor deposition (CVD) of thin TiO₂ films was studied on the macroscale level using a computational fluid model. The deposition rate was established for various substrate temperatures, showing the transition from a surface reaction rate limited regime to a mass limited regime.

© 2007 Elsevier B.V. All rights reserved.

1. Introduction

Thin TiO₂ films are industrially important materials due to a combination of properties, such as a high dielectric constant, a high refractive index, and high thermal stability [1,2]. The use of TiO₂ is established in e.g. heterogeneous catalysis, as a photocatalyst, as gas sensors, as a corrosion-protective coating, as an optical coating and in ceramics, see e.g. [3,4] and references therein.

The relevant processes for TiO₂ film deposition from titanium isopropoxide (TTIP) as a precursor can be described as [5]:

- heterogeneous reaction: $\text{TTIP}(\text{g}) \rightarrow \text{TTIP}(\text{ad}) \rightarrow \text{TiO}_2(\text{s}) + 4\text{C}_3\text{H}_6 + 2\text{H}_2\text{O}$
- intermediate reaction: $\text{TTIP}(\text{g}) \rightarrow \text{TiO}_2(\text{g}) \rightarrow \text{TiO}_2(\text{s})$
- homogeneous reaction: $\text{TTIP}(\text{g}) \rightarrow \text{TiO}_2(\text{p}) \rightarrow \text{TiO}_2(\text{s})$

where (g) is “gas”, (ad) is “adsorbed”, (s) is “solid” and (p) is “particle”. Particle formation in the gas phase (homogeneous reaction) will only occur at temperatures higher than 800 K [5]. Note that these reactions are global reactions, including numerous ‘true’ reactions. The real chemical pathways involved, however, are today essentially unknown.

The deposition of TiO₂ films from TTIP has already been studied extensively experimentally, see e.g. [2,7–11]. Also,

theoretical models were developed to investigate the growth of TiO₂–Pt thin films [12], and the synthesis of titania nanoparticles [13]. To our knowledge, however, the CVD of TiO₂ films from TTIP under atmospheric pressure CVD conditions has not been modeled numerically yet. Therefore, in this paper, we present the computational study of the deposition of thin TiO₂ films from atmospheric pressure CVD.

2. Description of the model

The simulations were performed for a so-called plug-down type of reactor, using the computational fluid dynamics approach. The reactor consists of two cm-scale cylinders: the gas flows in through the inner cylinder, and flows out through the outer cylinder, as indicated by the arrows in Fig. 1. Relevant chemical reactions were selected on the basis of the literature and implemented in the simulation. These reactions include two volumetric and two surface reactions, as given in Table 1.

The second surface reaction (i.e., reaction 4 of Table 1) is the direct chemisorption of gas phase TiO₂ molecules on the surface, as reported by Lee [5]. However, we did not find any quantitative data for this reaction. Hence, we have assumed identical parameters for this reaction as for the first surface reaction. To check the validity of this assumption, we have varied the kinetic parameters for the second surface reaction, as will be discussed below. The simulations were carried out for atmospheric pressure conditions, using N₂ as the carrier gas without oxidizing agent. The inlet gas velocity was set to 0.1 m/s.

* Corresponding author. Tel.: +32 3 820 23 82; fax: +32 3 820 23 76.
E-mail address: erik.neyts@ua.ac.be (E. Neyts).

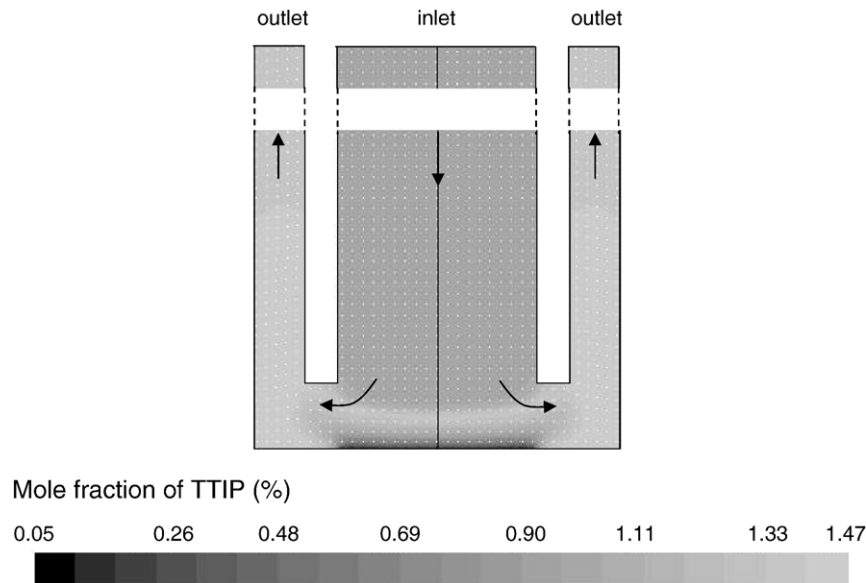


Fig. 1. Calculated mole fraction of TTIP in the reactor for a substrate temperature of 673 K.

The computational program used to model the fluid dynamics of the system is the commercially available software package Fluent 6.2 [6]. It utilizes the finite volume method to solve the governing equations, i.e., conservation of total mass, momentum, and energy, and the individual species conservation equations.

The reactive flow is modeled using the 2D axisymmetric laminar finite-rate model, including the above-mentioned volumetric and surface reactions. The final solution is obtained using the segregated solver. The Simple method for pressure-velocity coupling and the second order upwind scheme to interpolate the variables on the surface of the control volume were selected. The model reactor consists of in total 95,200 quadrilateral cells.

3. Results and discussion

3.1. Species concentrations in the reactor

The energy needed to overcome the activation energy of the volumetric reactions is provided by the heated substrate. The volumetric reactions give rise to the formation of $\text{TiO}_2(\text{g})$ and the depletion of TTIP. The calculated mole fractions of TTIP

and $\text{TiO}_2(\text{g})$ are illustrated in Figs. 1 and 2, respectively, for a substrate temperature of 673 K. The inlet mole fraction of TTIP was chosen to be 1%. Near the inlet, the gas temperature is 413 K, too low for the decomposition reaction (reaction 1 in Table 1) to take place. Since this reaction does not occur in this area of the reactor, no H_2O is created that is needed for the hydrolysis reaction to occur (reaction 2). Near the substrate, however, the gas temperature quickly rises to 673 K, such that TTIP is decomposed into TiO_2 , H_2O and C_3H_6 , resulting in the formation of TiO_2 gas molecules.

As can be seen in Fig. 1, the TTIP mole fraction first increases, and then decreases due to the gas phase decomposition and the surface reaction. The increase is caused by the gas flow carrying along the constituent TTIP and N_2 molecules. The N_2 molecules can easily follow the curvature of the gas flow and are pushed sideways. The heavier TTIP molecules, on the other hand, are characterized by a higher inertia and flow somewhat further down the reactor, before being carried along with the gas flow. Hence, a maximum of 1.3% is formed in the TTIP mole fraction. Quickly after this maximum, the gas temperature becomes high enough for the gas phase decomposition reaction to occur with the formation of $\text{TiO}_2(\text{g})$, and the TTIP mole fraction starts to decrease again.

The resulting mole fraction of $\text{TiO}_2(\text{g})$ is shown in Fig. 2. It increases from zero at the inlet, until a maximum at the centerline of 0.2% is reached at a distance of about 1 mm from the substrate. At the same time, however, both TTIP and $\text{TiO}_2(\text{g})$ near the substrate can react at the surface with the formation of solid TiO_2 . This explains why after this maximum the $\text{TiO}_2(\text{g})$ mole fraction drops again in the x-direction (i.e., in the direction of the gas flow).

Hence, TTIP is lost and TiO_2 is formed by both volumetric reactions, and both species are lost by one surface reaction. These reactions lead to the concentration profiles discussed above, co-determining the TiO_2 deposition rate.

Table 1

Chemical reactions implemented in the model. The pre-exponential factors in the gas phase reactions are given in units of s^{-1} and those of the surface reactions in m s^{-1}

Nr.	Reaction	Type	Arrhenius equation	Ref.
1	$\text{TTIP} \rightarrow \text{TiO}_2 + 2\text{H}_2\text{O} + 4\text{C}_3\text{H}_6$	Volumetric decomposition	$k_1 = 3.96 \times 10^5 \exp(-70.5/RT)$	[6]
2	$\text{TTIP} + 2\text{H}_2\text{O} \rightarrow \text{TiO}_2 + 4\text{C}_3\text{H}_7\text{OH}$	Volumetric hydrolysis	$k_2 = 3.0 \times 10^{15} \exp(-8.43/RT)$	[7]
3	$\text{TTIP} \rightarrow \text{TiO}_2(\text{s}) + 2\text{H}_2\text{O} + 4\text{C}_3\text{H}_6$	Surface deposition by TTIP	$k_3 = 1.0 \times 10^9 \exp(-126.01/RT)$	[8]
4	$\text{TiO}_2(\text{g}) \rightarrow \text{TiO}_2(\text{s})$	Surface deposition by TiO_2	$k_4 = 1.0 \times 10^9 \exp(-126.01/RT)$	[5]

Activation energies are given in units of kJ mol^{-1} .

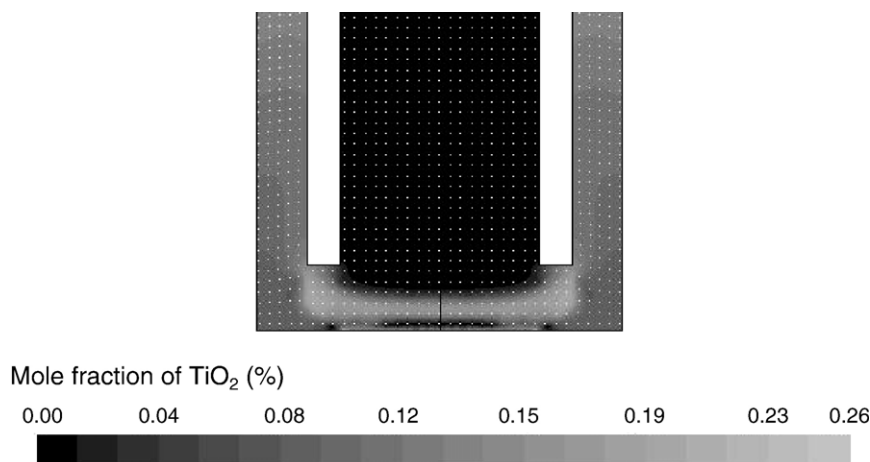


Fig. 2. Calculated mole fraction of $\text{TiO}_2(\text{g})$ in the reactor for a substrate temperature of 673 K.

3.2. TiO_2 deposition rate and the effect of the substrate temperature

In order to find out under which conditions optimal film deposition can be obtained, we have varied the substrate temperature, and investigated its effect on the deposition rate. In Fig. 3, the calculated average growth rate of $\text{TiO}_2(\text{s})$ (i.e., averaged over the substrate area), as well as the growth rates by the individual reactions, is plotted as a function of temperature, in the range 573–973 K.

It is clear from Fig. 3 that a maximum in the growth rate (of about $9 \mu\text{m}/\text{min}$) is found at a temperature of about 723 K. Below this temperature, the growth rate increases with the temperature, indicating that the growth is kinetically controlled. In this lower temperature region, the deposition rate is determined by the surface reactions, and both surface reactions show

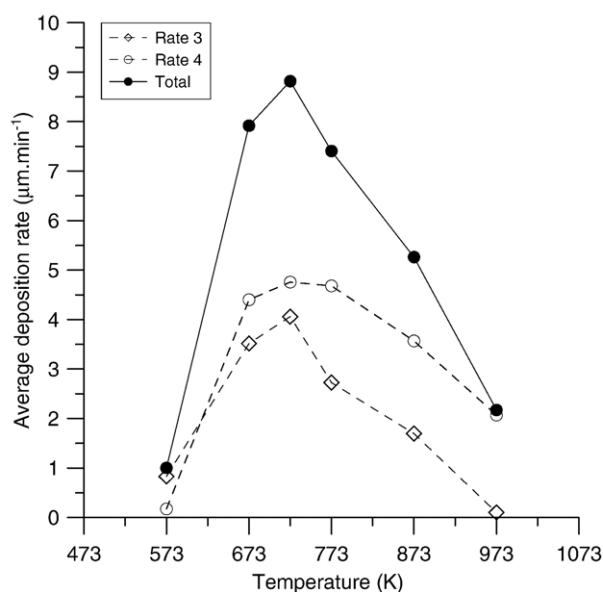


Fig. 3. Calculated total deposition rate of $\text{TiO}_2(\text{s})$ at the substrate, and contributions of the TTIP surface reaction (reaction 3 in Table 1) and the $\text{TiO}_2(\text{g})$ surface reaction (reaction 4 in Table 1), for various substrate temperatures in the range 573–973 K.

an increasing rate with temperature. Reaction 3 accounts for about 83% of the growth at a temperature of 573 K. The overall deposition rate at this temperature is calculated to be very low, about $1 \mu\text{m}/\text{min}$.

The maximum growth rate at a temperature of 723 K can be explained because at higher temperatures, the TTIP molecules can easily decompose, leading to a TTIP depletion near the substrate (see Fig. 1). As a result, the rate of reaction 3 (chemisorption of TTIP molecules) decreases with increasing temperature. Hence, the contribution of reaction 3 to the total deposition becomes mass limited. Also the rate of reaction 4 decreases with increasing temperature above 723 K. This can be explained as follows. As the temperature increases, the depletion of TTIP in the gas phase starts earlier in space. Hence, the maximum in the $\text{TiO}_2(\text{g})$ is also found earlier. It is indeed observed that the fraction of $\text{TiO}_2(\text{g})$ reaching the substrate decreases with increasing temperature. We therefore believe that more $\text{TiO}_2(\text{g})$ is carried away by the gas flow. Hence, also reaction 4 becomes mass limited at substrate temperatures above 723 K. Therefore, the overall deposition rate decreases with temperature above 723 K.

Although the rates of both surface reactions increase with temperature below 723 K, and decrease with increasing temperature above 723 K, their relative contributions change as a function of the substrate temperature. At 573 K, TTIP chemisorption was calculated to account for about 83% of the deposition, but at 723 K, it accounts for only 46%, and this value drops further to about 5%, at the highest substrate temperature investigated (973 K). It can therefore be expected that different types of films will be deposited at these different temperatures. This will be investigated in future work, where we will try to compare with experimental data, as soon as they will become available.

The film growth rate dependence on the substrate temperature is in good agreement with experimental data: an experimentally determined maximum in the growth rate was reported at a temperature of about 673 K [2], corresponding satisfactorily with the calculated maximum in the present simulations. The calculated abrupt depletion of the TTIP gas molecules with increasing temperature above about 673 K is also confirmed by their IR experiments [2].

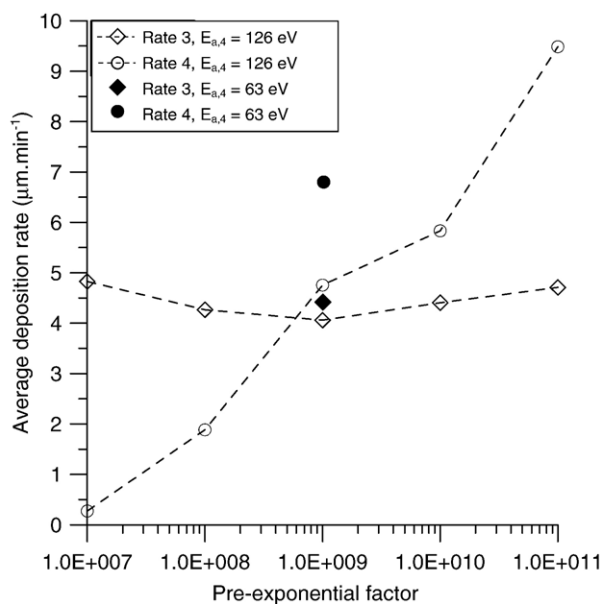


Fig. 4. Calculated contributions of reactions 3 and 4 to the total deposition rate for a substrate temperature of 723 K, as a function of varying the pre-exponential factor. Also indicated are the contributions of both reactions for an activation energy of 63 eV and a pre-exponential factor of $1.0 \times 10^9 \text{ s}^{-1}$ for reaction 4.

3.3. Effect of reaction parameters

As mentioned above, due to a lack of data, the reaction parameters of reaction 4 were assumed to be equal to those of reaction 3. To check the validity of this assumption, we have varied the value of the pre-exponential factor over 5 orders of magnitude for a substrate temperature of 723 K. The deposition rate due to both reactions is plotted in Fig. 4 as a function of the value for the pre-exponential factor of reaction 4. Furthermore, also the activation energy for reaction 4 was varied for a pre-exponential value of 10^9 s^{-1} .

It should be realized that at this temperature, the rate of reaction 4 is still surface reaction rate limited when using a pre-exponential value of 10^9 s^{-1} . It can be seen from the figure that the rate of this reaction remains surface reaction rate limited over the entire range of pre-exponential factors investigated.

Changing the pre-exponential factor of reaction 4 did not influence the rate of reaction 3. Hence, it only affects the relative

contribution of reaction 4 to the total deposition rate. Decreasing the activation energy for reaction 4 from 126 eV to 63 eV has the same effect as increasing the pre-exponential factor, i.e., increasing the reaction rate of reaction 4. The rate of reaction 3 is unaffected by the change in activation energy of reaction 4.

It should be mentioned that although the exact numbers of total deposition rate and relative contribution of reaction 4 to the total deposition rate are dependent on the specific kinetic parameters chosen, the mechanisms as described above and the qualitative trends remain essentially valid.

4. Conclusion

Simulations of thin amorphous TiO_2 films from TTIP were carried out for atmospheric pressure CVD conditions. The simulations show that a maximum growth rate is obtained at a substrate temperature of 723 K. At lower temperatures, growth is limited by the surface reaction rates, while at higher temperatures, growth proceeds in the mass limited regime.

Acknowledgment

The authors would like to thank the IWT for financial support.

References

- [1] Y.-M. Wu, D.C. Bradley, R.M. Nix, Appl. Surf. Sci. 64 (1993) 21.
- [2] K.-H. Ahn, Y.-B. Park, D.-W. Park, Surf. Coat. Technol. 171 (2003) 198.
- [3] U. Diebold, Surf. Sci. Reports 48 (2003) 53.
- [4] U. Diebold, N. Ruzycski, G.S. Herman, A. Selloni, Catal. Today 85 (2003) 93.
- [5] H.-Y. Lee, H.-G. Kim, Thin Solid Films 229 (1993) 187.
- [6] <http://www.fluent.com>.
- [7] K. Okuyama, R. Ushio, Y. Kousaka, R.C. Flagan, J.H. Seinfeld, AIChE J. 36 (1990) 409.
- [8] T. Seto, M. Shimada, K. Okuyama, Aerosol Sci. Technol. 23 (1995) 183.
- [9] G.A. Battiston, R. Gerbasi, M. Porchia, A. Gasparotto, in: M.D. Allendorf, C. Bernard (Eds.), Proceedings of the Fourteenth International CVD Conference and EUROCVD-11, 97, Electrochemical Society, Pennington, NJ, 1997, p. 660.
- [10] P. Babelon, A.S. Dequiedt, H. Mostéfa-Sba, S. Bourgeois, P. Sibilot, M. Sacilotti, Thin Solid Films 322 (1998) 63.
- [11] F.-D. Duminica, F. Maury, F. Senocq, Surf. Coat. Technol. 118 (2004) 255.
- [12] G.A. Battiston, R. Gerbasi, M. Porchia, A. Gasparotto, Chem. Vap. Depos. 5 (1999) 13.
- [13] S. Tsantilis, H.K. Kammler, S.E. Pratsinis, Chem. Eng. Sci. 57 (2002) 2139.